INFECTION AND IMMUNITY, May 1996, p. 1548–1558 Vol. 64, No. 5
0019-9567/96/$04.00+0

Chronic Proliferative Hepatitis in A/JCr Mice Associated with Persistent *Helicobacter hepaticus* Infection: a Model of Helicobacter-Induced Carcinogenesis

J. G. FOX,* X. LI, L. YAN, R. J. CAHILL, R. HURLEY,† R. LEWIS,‡ AND J. C. MURPHY

Division of Comparative Medicine, Massachusetts Institute of Technology, Cambridge, Massachusetts

Received 8 December 1995/Returned for modification 25 January 1996/Accepted 1 February 1996

Helicobacter hepaticus **causes hepatitis in selected strains of mice and in A/JCr mice is linked to liver cancer. To analyze whether *H. hepaticus* persists in specified ecological niches, to determine whether biomarkers of infection exist, and to analyze the influence of *H. hepaticus* on hepatocyte proliferation, a longitudinal study of *H. hepaticus*-infected A/JCr mice was undertaken. A/JCr mice were serially euthanatized from 3 through 18 months and surveyed by enzyme-linked immunosorbent assay; bacterial culture of liver, colon, and cecum; histology; electron microscopy; hepatocyte proliferation indices determined by using 5-bromo-2′-deoxyuridine; and measurement of the liver enzyme alanine aminotransferase. In infected animals throughout the 18-month study, *H. hepaticus* was consistently isolated from the lower bowel but only sporadically from the liver. By electron microscopy, *H. hepaticus* was noted infrequently and only in bile canaliculi. Infected mice, particularly males, showed chronic inflammation; oval cell, Kupffer cell, and Ito cell hyperplasia; hepatocytomegaly; and bile duct proliferation. The inflammatory and necrotizing lesion was progressive and involved the hepatic parenchyma, portal triads, and intralobular venules. Hepatic adenomas were noted only in male mice, whereas 5-bromo-2′-deoxyuridine proliferation indices were markedly increased in both sexes, but especially in males, compared with control A/J mice. Infected mice also developed sustained anti-*H. hepaticus* serum immunoglobulin G antibody responses and elevated alanine aminotransferase levels. *H. hepaticus*, which persists in the lower bowels and livers of A/JCr mice, is associated with a chronic proliferative hepatitis, and hepatomas in selected male mice indicate that this novel bacterium may cause an increased risk of hepatic cancer induction in susceptible strains of mice. This murine model should prove useful in dissecting the molecular events operable in the development of neoplasms induced by bacteria belonging to this expanding genera of pathogenic *Helicobacter* species.**

A new helical bacterium was observed recently in the livers of several strains of inbred mice which originated from a barrier-maintained facility at the National Cancer Institute in Frederick, Md. (50). The bacterium was subsequently isolated and named *Helicobacter hepaticus* on the basis of its morphology, biochemistry, and 16S rRNA sequence (21). The bacterium is associated with a chronic active hepatitis in a variety of mouse strains, including A/JCr, BALB/CAnNCr, SJL/NCr, SCID/NCr, and C3H/HeNCr (50). C57BL/6NCr mice appear to be resistant to the ability of *H. hepaticus* to produce liver lesions. In 18-month-old A/JCr mice, which normally have a very low incidence of hepatitis and hepatic tumors, the *H. hepaticus*-associated chronic hepatitis was linked with the occurrence of hepatocellular tumors in a high proportion of the control animals in a bioassay study (50). In these studies, the actual presence of the bacteria was based on morphological evidence only. Preliminary evidence also indicated that the organism could induce hepatitis in naive A/J mice when a liver homogenate containing *H. hepaticus* was injected intraperitoneally (50). A newly recognized related bacterium, *H. bilis*, is also associated with hepatitis in aged inbred strains of mice, but it is not known whether this helicobacter causes liver tumors (24).

Because *H. hepaticus* infection in A/JCr mice offers a potentially exciting animal model with which to study *Helicobacter*-associated hepatic cancer, we wanted to ascertain whether *H. hepaticus*-infected A/JCr mice housed under different conditions developed liver lesions similar to those noted in this strain of mice previously maintained at the National Cancer Institute (48, 50). Also, the aim of the study was to determine by culture whether *H. hepaticus* could be isolated on a longitudinal basis from intestines and livers of infected mice. These findings were correlated with a progression of liver pathology and measurement of hepatocyte proliferation by 5-bromo-2′-deoxyuridine (BrdU) in mice of different ages and compared with findings for A/J mice not infected with *H. hepaticus*. The mice were also monitored for immunoglobulin G (IgG) serum antibody to *H. hepaticus* as well as for elevation of a liver enzyme, alanine aminotransferase (ALT), a useful marker for damage of liver parenchyma in human hepatitis and liver disease in transgenic mice expressing hepatitis B viral antigens (5).

* Corresponding author.

† Present address: Center for Research Animal Resources, New York State College of Veterinary Medicine, Cornell University, Ithaca, N.Y.

‡ Permanent address: Department of Veterinary Pathology, New York State College of Veterinary Medicine, Cornell University, Ithaca, N.Y.

MATERIALS AND METHODS

Longitudinal study. A total of 90 *H. hepaticus*-infected, viral-antibody-free mice were examined over the length of the study. Five male and five female pups were born at the Massachusetts Institute of Technology from *H. hepaticus*-infected A/JCr dams and were euthanatized with CO_2 at 3 months of age. Forty (20 male, 20 female) A/JCr mice were received at the Massachusetts Institute of Technology from the National Cancer Institute as weanlings and in groups of 5 males and 5 females were euthanatized at 6, 8, 9, and 10 months of age. Another

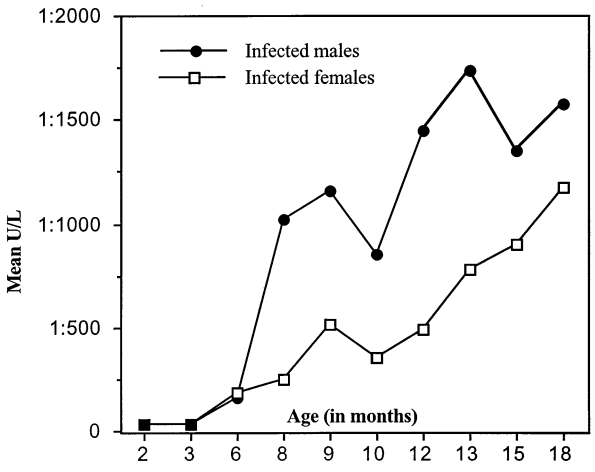

FIG. 1. *H. hepaticus* IgG ELISA levels in infected A/JCr and control A/J mice.

40 A/JCr mice arrived at 7 to 8 months of age and were killed at 12 months (5 female, 5 male), 13 months (7 female, 10 male), 15 months (5 female, 1 male), and 18 months (4 female, 3 male). Thirty control A/J mice determined to be free of *H. hepaticus* by culture were euthanatized at 8, 10, and 13 months of age (5 male and 5 female at each time point) for BrdU, pathology analysis, and measurement of *H. hepaticus* IgG serum antibody and ALT.

The infected A/JCr and control A/J mice were housed separately in American Association for Accreditation of Laboratory Animal Care-approved facilities at the Massachusetts Institute of Technology. The A/JCr mice were maintained in microisolator cages with hardwood bedding, fed commercial pelleted rodent diet (Agway, Waverly, N.Y.), and given water ad libitum. The A/J mice were maintained similarly but were housed less than 1 week prior to euthanasia.

***H. hepaticus* isolation.** Intestinal scrapings of the cecum and colon and a liver specimen collected aseptically were cultured for *H. hepaticus*. Bacterial isolation from infected mice was performed on trimethoprim-vancomycin-polymyxin (Remel Laboratories) blood agar plates at 37°C under microaerobic conditions in vented jars containing N_2, H_2, and CO_2 (90:5:5). Colonic and cecal contents were filtered through a 0.45-μm-pore-size filter prior to culture on trimethoprim-vancomycin-polymyxin agar (14, 40). Characteristic colonies were Gram stained, and bacteria were examined for morphology and size. Viable bacteria were also examined by phase microscopy for motility. Oxidase, catalase, and urease reactions and sensitivity to nalidixic acid and cephalothin were also determined (21).

Enzyme-linked immunosorbent assay (ELISA) for anti-*H. hepaticus* antibody.
(i) Animals. A/JCr mice were anesthetized with methoxyflurane for collection of blood via orbital bleeding. Groups of A/JCr male and female mice were bled at 3- to 4-month intervals and then bled under CO_2 anesthesia prior to euthanasia (Fig. 1). The A/J mice were bled once under CO_2 anesthesia prior to being euthanatized.

(ii) Antigen preparation. *H. hepaticus* sonicate for use in the ELISA was prepared similarly to *H. felis* sonicate described elsewhere (18). In brief, *H. hepaticus* was grown for 96 h in *Brucella* broth (Difco Laboratories, Detroit, Mich.) containing 5% fetal calf serum. Cultures were incubated at 37°C in a microaerobic environment and were shaken at 10,000 rpm (Sorvall RC-5B; Dupont, Newtown, Conn.) for 10 min, and the pellet was washed three times in phosphate-buffered saline (PBS). The pellet was then diluted in PBS to an optical density (600 nm) of ~1.0, and the bacterial cells were disrupted by sonication (Artec K System Inc., Farmingdale, N.Y.). After centrifugation at 10,000 rpm for 10 min, the protein content was determined. Aliquots were frozen at −70°C until used in the assay.

(iii) ELISA. The ELISA was performed as previously described (18, 23). Wells of microtiter plates (Dynatech Laboratories, Chantilly, Va.) were incubated with 100 ng of *H. hepaticus* protein per ml in carbonate buffer. After the plates were washed, serial twofold dilutions of sera from *H. hepaticus*-infected or control mice were incubated for 60 min at 37°C; the appropriate dilution of alkaline phosphatase-conjugated goat anti-mouse IgG (Sigma, St. Louis, Mo.) was then added to each well. Serum IgG antibody titers of <1:64 were considered negative.

(iv) ALT liver enzyme analysis. Serum ALT was measured on a longitudinal basis in A/JCr mice and at one time point in A/J controls, using sera from the same mice in which the *H. hepaticus* ELISA was performed. A 10-μl drop of serum was deposited on a multilayered film supported in plastic according to manufacturer's instructions (Kodak Ektachem DT slide; Eastman Kodak Co., Rochester, N.Y.). The analysis is based on an enzyme-coupled oxidation of NADH to NAD^+. The rate of oxidation was monitored by reflectance spectrophotometry and was used to measure ALT activity.

Pathology. A complete necropsy was performed, and liver samples were taken from the left lateral, left middle, right middle, and quadrate lobes of each mouse. A longitudinal section was made from apical or free margin to the hilus of each lobe. Each lobe was cut in different lengths, left lateral > right middle > left middle > quadrate lobes, to ensure the identification of each lobe on microscopic examination. The intestinal tract of each animal was also examined. The liver lesions were examined, and the liver damage was classified according to the following criteria: extent and type of inflammatory cell infiltrates in the parenchyma, periportal and perivenous areas; oval cell and bile ductular hyperplasia; Kupffer cell hyperplasia; and hepatocellular pleomorphism. The parameter of each of these lesions was graded semiquantitatively as 0 (none), 1 (minimal), 2 (mild), 3 (moderate), and 4 (severe) in the liver. The score from each parameter was accumulated for each mouse and then averaged by sex for each age group.

For histopathology, tissues were fixed in 10% neutral buffered formalin for 24 h, embedded in paraffin, cut at 5 μm, and stained with hematoxylin-eosin and Warthin-Starry methods. Additional 5-μm sections were cut from BrdU-labeled liver samples from mice aged 8, 10, and 13 months and mounted on the siliconized Probe-On Plus slides (Fisher, Pittsburgh, Pa.) for BrdU detection by immunohistochemistry.

Electron microscopy. Selected liver samples were fixed in Karnovsky's fixative, postfixed with 1% osmium tetroxide, dehydrated through graded acetone, and embedded in Epon-araldite 6005 mixture (33). The plastic blocks were cut into 1-μm-thick sections and stained with methylene blue-azure II. The areas of interest were identified under a light microscope, cut from the plastic block, and mounted into a plastic bean capsule. A 50- to 70-nm-thick section was then cut, stained with uranyl acetate-lead citrate, and visualized with a transmission electron microscope.

BrdU labeling. BrdU labeling was performed as described previously for labeling proliferating hepatocytes in mice (10, 47). Ten mice in each age group (8, 10, and 13 months) were injected intraperitoneally with 0.56 mg of BrdU per day for 5 days for both control and infected mice. Four hours after the last injection on day 5, the animals were euthanatized with CO_2. Briefly, tissue sections mounted on the Probe-On Plus slides were deparaffinized by three changes of xylene and rehydrated through graded ethanol. The sections were washed three times in distilled water, and the endogenous tissue peroxidase was quenched by incubating the sections in aqueous 3% H_2O_2 for 15 min at room temperature. After being washed three times in PBS, the section was incubated in 0.1% trypsin, 1 N HCl, anti-BrdU antibody working solution at 1:100 dilution, and peroxidase-conjugated anti-mouse IgG antibody (Sigma) sequentially at 37°C for 30 min. The section was washed with PBS between each incubation. After being rinsed with PBS, the sections were covered with freshly prepared diaminobenzidine solution (Kirkegaard & Perry, Gaithersburg, Md.) for 10 to 15 min at room temperature. Sections were rinsed with PBS, counterstained with hematoxylin, dehydrated through the graded ethanol, rinsed clear in xylene, and mounted permanently.

The sections from each mouse were recoded randomly, without knowledge of animal identifications or treatment groups. Incorporation of BrdU labeling was quantified by counting labeled nuclei among a minimum of 1,000 hepatocytes for 20 high-powered fields (40×), with a minimum of five high-powered fields per lobe (caudate, left lateral, right middle, and right lateral). A positive labeling score was ascribed for hepatocytes with brown-staining nucleus and clear cytoplasm, regardless of the staining intensity. Binucleated hepatocytes were counted as one cell. Results were expressed as mean number of cells per high-powered field, mean number of labeled cells per high-powered field, and labeling index percent (LI%) per high-powered field for each lobe and for the entire liver (mean of all four lobes). LI% was calculated by dividing the total number of labeled hepatocytes per high-powered field by the total number of hepatocytes in that field and expressing the result as a percentage. A piece of tissue that has a high cell turnover ratio, i.e., duodenum, gastric mucosa, or spleen, was included in each section as a positive control. Negative controls were included in each assay and were performed by replacing the primary antibody with normal mouse serum. After the evaluations were completed, the codes were broken and mean hepatocyte labeling index was calculated for each liver lobe.

Rabbit immunization. A rabbit was immunized with a whole cell sonicate of *H. hepaticus* (280 μg of protein per immunization). The whole cell sonicate was prepared from a washed pellet of an *H. hepaticus* broth culture. The pellet was suspended in PBS, and the cells were disrupted by three cycles of sonication for 5 min followed by freezing and thawing. The sonicate was tested for sterility by phase microscopy, plating on blood agar plates, and incubation aerobically and microaerobically. The rabbit was immunized subcutaneously with an initial injection of 1 ml of antigen mixed with Freund's complete adjuvant (1:1, vol/vol) followed at 1 and 5 weeks with 1 ml of antigen in Freund's incomplete adjuvant (1:1, vol/vol). The rabbit was test bled at 4 and 8 weeks postimmunization.

An ELISA was carried out to determine the antibody response of the rabbit. Wells were coated with 1 μg of whole cell sonicate, and the ELISA was carried out as described previously (18, 20), using anti-rabbit IgG conjugated to alkaline phosphatase.

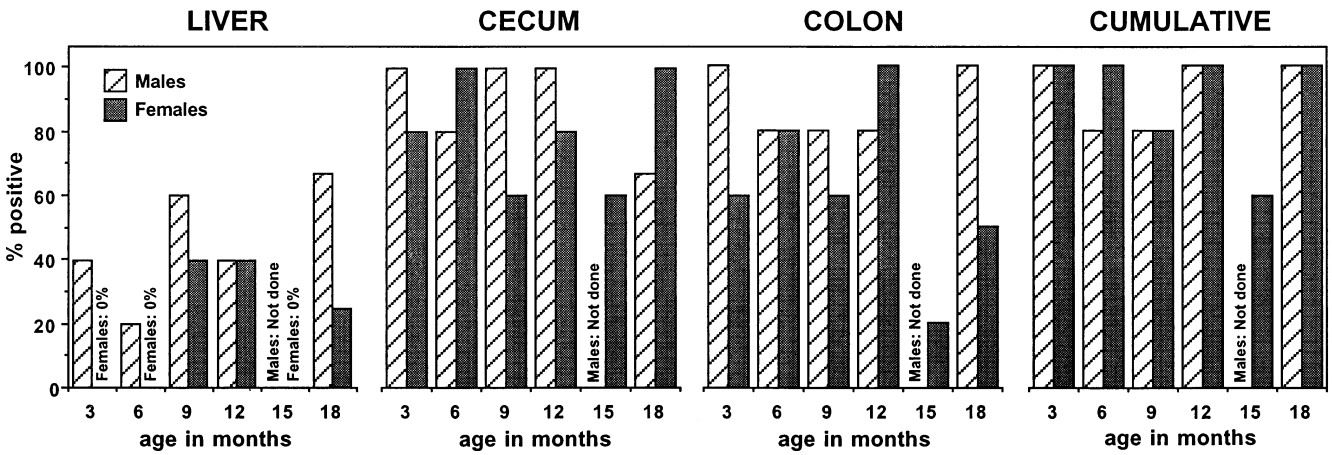

FIG. 2. *H. hepaticus* in A/JCr mice cultured on a longitudinal basis.

Immunofluorescence staining of A/J mice livers. Livers from 11 male A/JCr mice (3, 6, 8, 10, 13, and 18 months of age) and from control A/J mice were processed for immunofluorescence staining using polyclonal *H. hepaticus* rabbit antisera. Tissue sections were deparaffinized and rehydrated through xylene and ethanol to water. The slides were incubated with 0.05% pronase (Sigma P5147) for 30 min at 37°C and washed with PBS for 5 min. The tissue sections were covered with either rabbit preimmune serum or postimmune serum to *H. hepaticus* whole cell sonicate (both 1:100 in PBS) and incubated for 60 min at 37°C in a humid atmosphere. Slides were then washed twice in PBS (5 min each time), incubated for 30 min with anti-rabbit IgG-fluorescein isothiocyanate conjugate (1:50 in PBS; Sigma F0511) at 37°C, and rinsed in PBS for 5 min. The slides were mounted with coverslips and sealed with buffered glycerol. Slides were examined with a Zeiss fluorescence microscope.

Serum absorption with *H. hepaticus*. Polyclonal *H. hepaticus* antiserum (0.20 ml) was added to a pellet of PBS-washed (three times) *H. hepaticus* ($\sim 5 \times 10^8$ CFU) whole cells. The bacterial pellet was resuspended and incubated for 1 h at 37°C. The pellet was recentrifuged at 1,200 rpm for 10 min, and the serum was used for analysis of immunofluorescence staining of liver. In a second series of experiments, the bacterial pellet was resuspended and incubated with the polyclonal antiserum for two successive incubations at 37°C for 1 h. The serum was incubated in a similar manner with equal numbers of *Campylobacter jejuni* and *Escherichia coli* cells (i.e., 5×10^8) to test for specificity of absorption of *H. hepaticus* IgG antibodies.

RESULTS

Colonization of liver and intestinal tissue with *H. hepaticus*. The culture results for the isolation of *H. hepaticus* from infected mice are shown in Fig. 2. Cecal scrapings of infected male mice were 100% positive for *H. hepaticus* at 3, 9, 12, and 18 months, whereas *H. hepaticus* was recovered from the ceca at lower frequency in female mice, except at 6 and 18 months, at which ages 100% of the females were *H. hepaticus* positive. Isolation rates of *H. hepaticus* noted in colonic cultures were somewhat different, with 100% recovery rates in male mice at 3 and 18 months and in female mice at 12 months and 40 to 80% positive being recorded in males and females at other time points. *H. hepaticus* was recovered from the livers of 20 to 60% of male mice at each time point. *H. hepaticus* was not recovered from the livers of female mice at 3, 6, or 15 months and was recovered in only 40% of mice 9 and 12 months of age and 25% at 18 months. The cumulative percentage of *H. hepaticus*-infected mice, i.e., mice in which *H. hepaticus* was isolated from any one of the three sites, however, was consistently high. At 3, 12, and 18 months, *H. hepaticus* was isolated from at least one site in 100% of male and female mice; a 60% recovery was the lowest incidence recorded in females at 15 months.

***H. hepaticus* ELISA.** Detectable levels of *H. hepaticus* began to appear at 6 months in both males and females (Fig. 1). However, at 8 months, the ELISA values in males increased and plateaued at 12 months, whereas female ELISA values remained static at 8 to 12 months and then began to increase gradually to approach those of males at 18 months. The ELISA measurement in male mice versus female mice was significantly different at 9 ($P = 0.0003$) and 13 months ($P = 0.0001$) but not at 18 months ($P = 0.47$). *H. hepaticus* IgG was not detected in control A/J mice of both sexes.

ALT. ALT levels in *H. hepaticus*-infected A/JCr mice were below 100 IU at 2 to 3 months and in the males began to increase at 6 months to obtain a maximum level of 303 at 12 months, at which time the mean levels of ALT decreased to 178 and 134, respectively, at 13 and 15 months; at the 18-month level, the mice had again obtained a mean level of 294 IU, comparable to that recorded at 12 months of age. The female ALT level followed the same general pattern but was consistently lower at all time points. The highest mean level of ALT, 219 IU, was recorded in 8-month-old females. In control A/J mice, values were 201, 132, and 148 IU and 81, 128, and 70 IU in female and male mice at 8, 10, and 13 months, respectively.

Histopathology. Grossly, only a small portion (<10%) of the infected mice had single to multiple yellow to gray foci and/or prominent reticular patterns in one or more liver lobes. The foci varied from 1 to 3 mm in diameter, with occasionally coalescing foci. Single to multiple 1- to 3-mm-diameter, brown to gray, spherical nodules were observed in the liver parenchyma of one 12-month-old, two 13-month-old, and two 18-month-old male mice. The severity of histological changes in the livers of infected mice is shown in Fig. 3. Livers of male mice were more severely affected than those of female mice ($P < 0.05$).

The predominant changes in the livers from 3 to 6 months of age were multifocal to coalescing coagulative necrosis of the hepatocytes with variable infiltration of lymphocytes, macrophages, and neutrophils at the periphery (Fig. 4a). Sizes of the necrotic foci varied from a few to numerous hepatocytes. Inflammatory cell infiltration was mild and multifocal in the remaining parenchyma and periportal areas. From 8 to 10 months, infiltration of the inflammatory cells, hyperplasia or hypertrophy of Kupffer cells, Ito cells, and oval cells, and pleomorphism of the hepatocytes became prominent in the affected foci (Fig. 4B). Lymphocytes with variable numbers of plasma cells, macrophages, and neutrophils accumulated multifocally in the parenchyma and periportal and perivenous areas, especially around the bile ducts. The perivascular lesions were characterized by hepatocellular necrosis, lymphocytic and

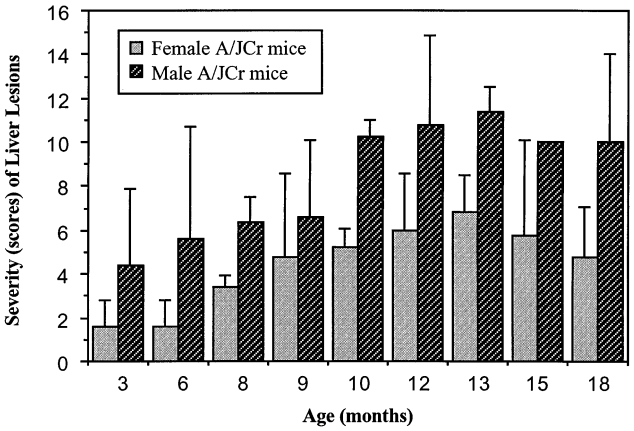

FIG. 3. Severity of liver lesions in A/JCr male and female mice from 3 through 18 months.

plasmacytic, and often neutrophilic inflammation which extended radially and irregularly from the center of the lesion into the hepatic parenchyma. Hepatic arterioles within the portal triads appear unaffected. Bile duct hyperplasia was seen in many portal areas (Fig. 4c). Epithelial erosion or ulceration and periductal lymphoid aggregation occurred in some bile ducts (Fig. 4d). Mild pericholangeal fibrosis was seen in some bile ducts. Some of the macrophages and Kupffer cells contained intracytoplasmic yellow to brown pigment. Hyperplastic oval cells radiated from the inflamed foci to adjacent hepatic parenchyma and sometimes bridged to adjacent portal areas, with occasional formation of bile ductules. Hepatocyte necrosis became less prominent, but collapse of hepatic plates and capsular surface due to the loss of hepatocytes was observed occasionally. Cytomegaly and karyomegaly of the hepatocytes became evident, with frequent intranuclear pseudoinclusions (Fig. 4b).

By 12 to 18 months of age, the changes occurring from 8 to 10 months became more advanced, and altered hepatocellular foci and adenomatous hepatocellular nodules appeared in some male mice. Single to multiple eosinophilic foci were observed in three mice at 12, four at 13, one at 15, and three at 18 months of age (Fig. 4e). Clear foci were observed in one mouse each at 12 and 13 months of age. The adenomatous nodules were observed in one male mouse at 15 months and two male mice at 18 months of age (Fig. 4f). The altered foci and nodules were often surrounded by the inflammatory cells.

Warthin-Starry and immunofluorescence-stained liver sections revealed spiral-shaped *H. hepaticus* cells in mice of all ages, except for female mice at 15 months of age (Fig. 5a and b). The bacteria appeared to be between the hepatocytes. Severity of the hepatic lesions in some cases correlated with the abundance of bacteria in the tissues. Mild nonsuppurative typhlitis was observed in some infected mice from 3 to 18 months of age (Fig. 5c). Organisms with morphology compatible with *H. hepaticus* were observed in the crypts of ceca of mice with or without typhlitis (Fig. 5d). However, severity of the typhlitis did not appear to be age or sex dependent. No lesions were observed in any tissues of the control mice.

Transmission electron microscopy. The hypertrophic hepatocytes contained abundant mitochondria and/or endoplasmic reticula. Cytoplasmic invagination into nuclei was frequently seen (intranuclear pseudoinclusions) (Fig. 6a). Ito cells had markedly vacuolated cytoplasm and displaced nuclei. The bacteria were observed within bile canaliculi of the infected mice (Fig. 6b). The affected canaliculi were variably dilated, with swelling, blunting, and decreased numbers of the canalicular microvilli.

BrdU labeling. Analysis of each lobe for total number of cells, number of labeled cells and LI% per high-powered fields showed no significant difference in the lobular distribution of proliferating cells within an animal, in both the mice infected with *H. hepaticus* and controls (Table 1). There was no significant change in hepatocyte proliferation (LI%) associated with age in control mice at 8, 10, and 13 months. Mice infected with *H. hepaticus* had a higher labeling index compared with controls at all time points (8, 10, and 13 months; Fig. 7 and Table 1). This difference was significant at 10 and 13 months ($P = 0.03$, $P = 0.005$) but did not reach significance at 8 months ($P = 0.053$). There was a trend toward increasing hepatocyte proliferation (LI%) in *H. hepaticus*-infected mice over time; this difference did not reach significance. The pattern of proliferation was different, however, at different time points. At 8 and 10 months, there was an increase in cell proliferation compared with controls, demonstrated by the increased LI%, without a significant difference in the total number of cells per high-powered field. At 13 months, there was a continued increase in cell proliferation as well as a significant decrease in the number of cells per high-powered field compared with infected animals at the earlier time points ($P = 0.031$). There was no significant difference between the numbers of labeled cells per high-powered field at each time point for infected mice, which were significantly higher than for control mice (Table 1).

When the study groups were subdivided according to gender, there was no significant difference between male controls and female controls at any time point. However, labeling indices were higher for male mice infected with *H. hepaticus* than for female infected mice at every time point, and this difference reached significance at 8 months ($P = 0.04$; Fig. 7). Male infected mice had a significantly higher LI% than male controls at all time points. There was no significant difference between the LI% of female mice infected with *H. hepaticus* and female controls at any time point. *H. hepaticus*, therefore, appears to exert more influence on hepatocyte proliferation in male than in female mice, which is consistent with the higher incidence of hepatic tumors in male than in female A/JCr mice.

In the infected mice, the BrdU-labeled hepatocytes were mostly aggregated within or adjacent to the inflammatory foci, proliferating nodule, and adenomatous masses (Fig. 6). In the control mice, the BrdU-labeled hepatocytes were randomly distributed within the parenchyma.

Immunofluorescence assay of liver. In the ELISA described earlier, the rabbit produced a serum IgG antibody titer in excess of 1:1,000 (18, 20). Livers subjected to immunofluorescence staining with *H. hepaticus* polyclonal rabbit antisera demonstrated focal accumulation of clearly identified fluorescent particulate to globular structures within the cytoplasm of hepatocytes (Fig. 5b). After absorption of the *H. hepaticus* rabbit polyclonal antisera with whole-cell *H. hepaticus* sonic extract, staining decreased or was eliminated entirely with single or double absorption, respectively, indicating specificity of the reaction (Table 2). Also, in 10 of the 11 mouse livers, *H. hepaticus* stained with the fluorescence-labeled *H. hepaticus* rabbit polyclonal antibody (Fig. 5b). This staining was also eliminated with preabsorption of the antisera with whole-cell sonicate of *H. hepaticus*. Specific *H. hepaticus* fluorescent staining of the endothelium of central venules was also noted. Cross-absorption of sera with *C. jejuni* or *E. coli* did not diminish specific immunofluorescence in the livers of *H. hepaticus*-infected mice.

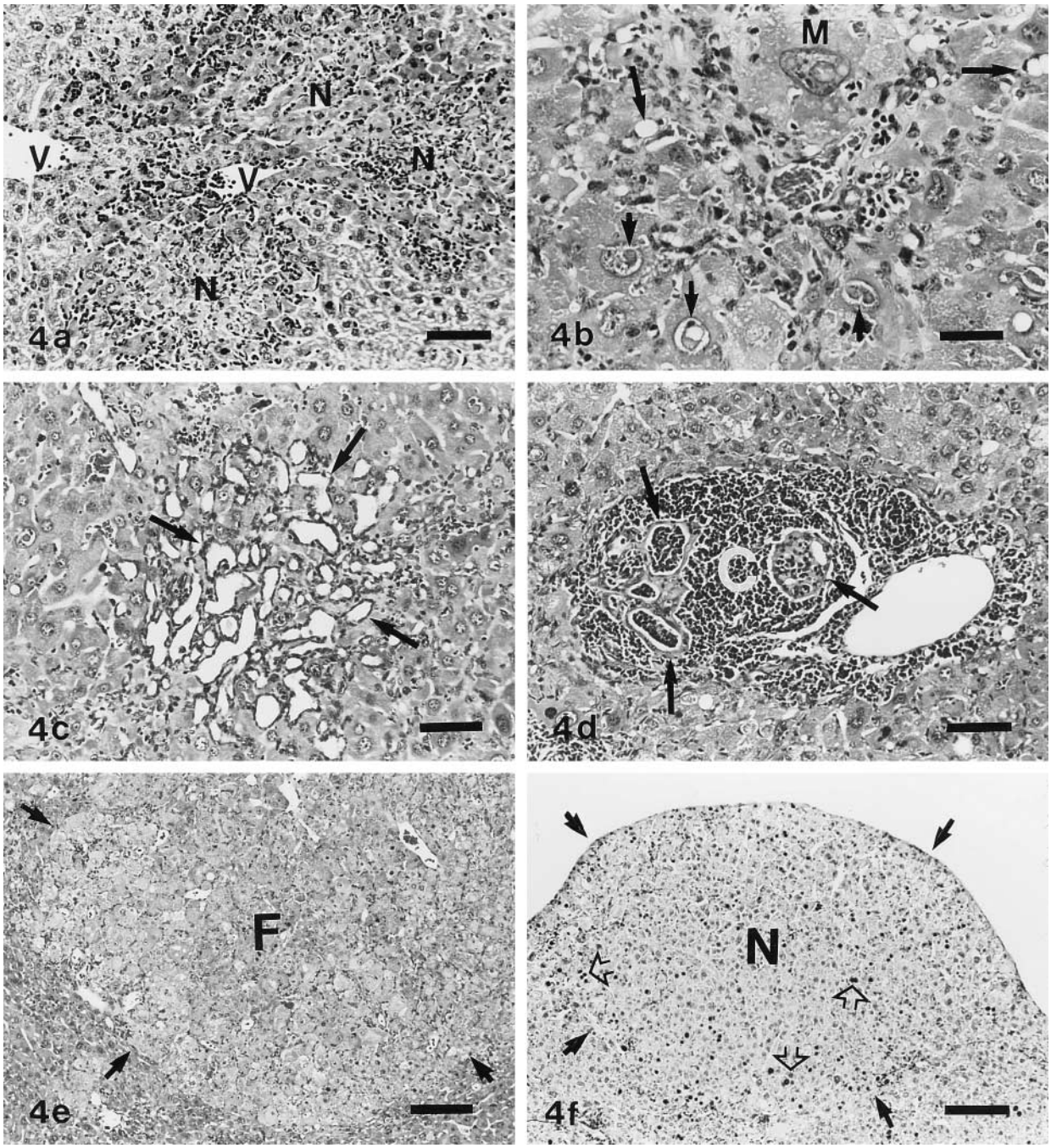

FIG. 4. (a) Liver, infected A/JCr mouse; coagulative necrosis (N) of hepatocytes and inflammatory cell infiltration in periportal and perivenous areas (V). Bar = 94 μm. (b) Liver, infected A/JCr mouse; hepatocytomegaly (M) surrounded by inflammatory cells, pseudoinclusions in hepatocyte nuclei (short arrows), and Ito cell hyperplasia or hypertrophy (long arrows). Bar = 46 μm. (c) Liver, infected A/JCr mouse; bile ductular hyperplasia (arrows) with inflammatory cell infiltration. Bar = 88 μm. (d) Liver, infected A/JCr mouse; bile duct hyperplasia (arrows) and portal inflammatory cell infiltration (C), with inflammatory cells in the ductal epithelia and ductal lumina. Bar = 90 μm. (e) Liver, infected A/JCr mouse. An altered hepatocellular focus (F) consists of large pale disorganized hepatocytes, with tinctorial changes of the cytoplasm and compression of the adjacent hepatic parenchyma (arrows). Bar = 160 μm. (f) Liver, infected A/JCr mouse. An adenomatous nodule (N) of proliferating hepatocytes projects onto capsular surface and compresses the adjacent hepatic parenchyma (solid arrows). Many of hepatocellular nuclei within the nodule are positively labeled with BrdU (open arrows). Bar = 168 μm.

DISCUSSION

Spiral-shaped bacteria have been observed in human and animal stomachs since the end of the last century (22, 31). In most instances, the gastric organisms were considered commensal because they did not invade the mucosa. However, *H. pylori* infection has a global distribution and is now known to cause gastritis and duodenal ulcers (2, 25, 26, 28, 34). Recently, epidemiologic studies indicate that *H. pylori*-associated gastritis in selected individuals can progress to gastric adenocarcinoma (6, 7, 15, 16, 38, 43, 44). Because of the widespread and persistent nature of *H. pylori* gastritis, a high proportion of humans are at a risk of gastric tumors (6, 8, 37, 38). The

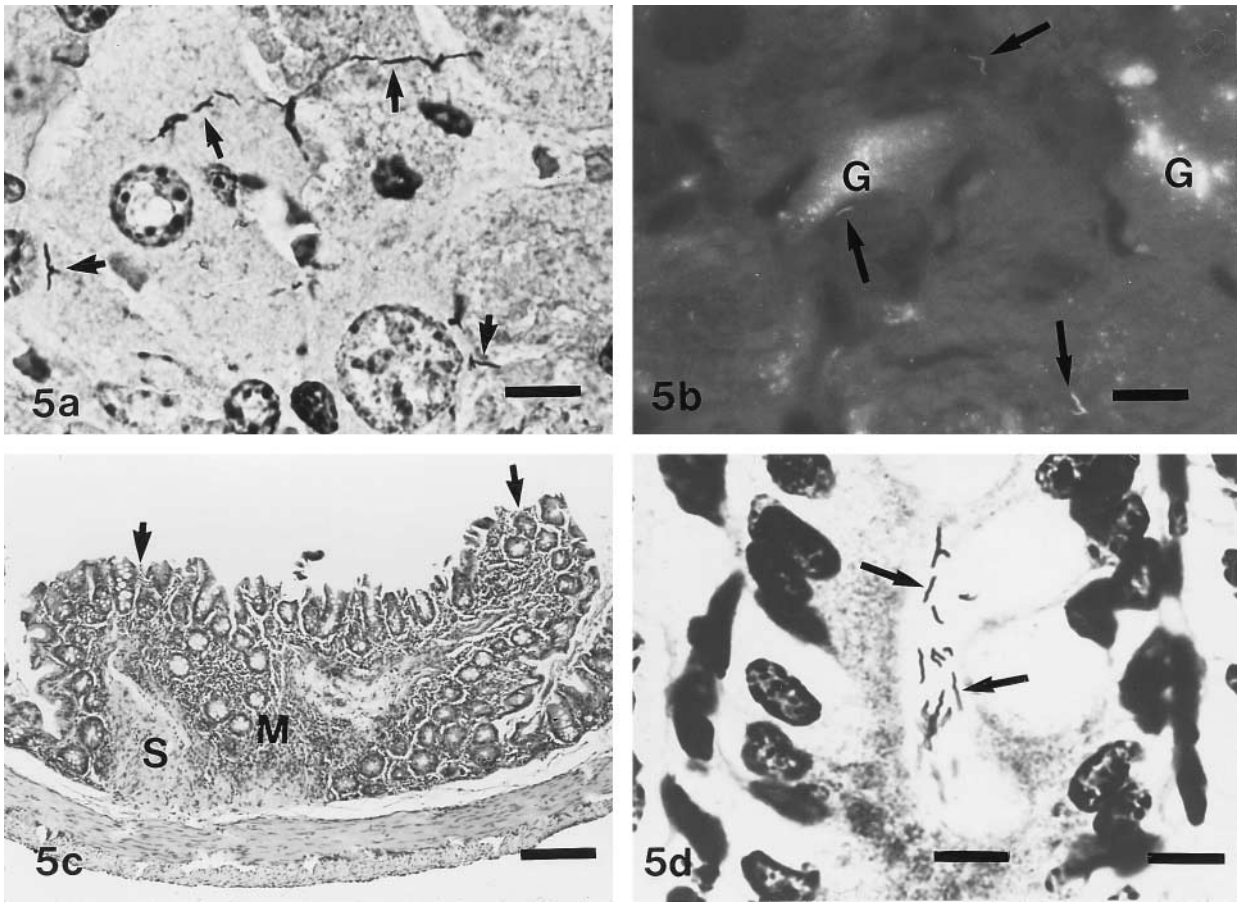

FIG. 5. (a) Liver, infected A/JCr mouse. Warthin-Starry stain reveals many spiral-shaped *H. hepaticus* cells within the hepatic parenchyma (arrows). Bar = 12 μm. (b) Liver, infected A/JCr mouse. Immunofluorescence staining with rabbit polyclonal *H. hepaticus* antisera reveals spiral-shaped *H. hepaticus* cells within the hepatic parenchyma (arrows) and positively stained granular material within some hepatocytes (G). Bar = 14 μm. (c) Cecum, infected A/JCr mouse; mild to moderate infiltration of inflammatory cells in the mucosa (M) and submucosa (S), with superficial erosions (arrows). Bar = 93 μm. (d) Cecum, infected A/JCr mouse. Warthin-Starry stain reveals many spiral-shaped organisms compatible with *H. hepaticus* morphology in the crypt (arrows). Bar = 9 μm.

organism is now considered a cofactor in induction of gastric cancer, and in one study it was shown to be implicated as an independent risk indicator for gastric tumors (27). Recently, *H. pylori* also has been linked to development of low-grade lymphoma (1, 52). However, the pathogenesis of the *H. pylori*-associated gastric malignancies in humans is virtually unknown. Many hypotheses have been proposed, and adequate animal models are still under development (17). As these in vivo model studies ensued, six additional *Helicobacter* species isolated from the stomachs of various mammals were shown to cause various degrees of gastritis in their hosts (22). *Helicobacter* species have also been isolated from the intestinal tracts of humans, animals, and birds (22). Recently, two intestinal helicobacters in mice, *H. hepaticus* and *H. bilis*, have been isolated from diseased livers of inbred and outbred mice (21, 24).

This study clearly determined that persistent infection with *H. hepaticus* correlated with hepatic disease in A/JCr mice. Although liver lesions were consistently present in the different A/JCr age groups, albeit more commonly in older male mice, isolation of *H. hepaticus* from livers of these mice was sporadic, whereas *H. hepaticus* was consistently cultured from the ceca or colons of mice with or without significant hepatitis. Failure to isolate *H. hepaticus* from livers of infected mice may be due to small numbers of bacteria present in hepatic parenchyma, difficulty of culturing small numbers of this fastidious bacterium, or presence of *H. hepaticus* growth inhibitors in mouse livers. Even though use of the Warthin-Starry and immunofluorescent stains facilitated visualization of organisms, bacteria were still difficult to identify and, when present, were often restricted to the periphery of areas of hepatic necrosis. This finding is consistent with our findings and earlier observations of others (48, 50). Nevertheless, we established that in 100% of the mice surveyed during this longitudinal study, *H. hepaticus* was isolated from either the cecum or colon. Thus, for routine diagnosis of *H. hepaticus* in infected mice, we recommend that isolation be attempted from the lower intestine, not the liver parenchyma. Furthermore, *H. hepaticus* culture from infected mice is facilitated by filtering feces or intestinal contents through a 0.45-μm-pore-size filter, a technique used successfully to isolate other intestinal helicobacters and campylobacters (14, 40).

The epidemiology of *H. hepaticus* infection is unknown; however, the persistent infection of the lower intestine with *H. hepaticus* strongly supports the premise that the disease is transmitted by fecal-oral spread, particularly when the coprophagic nature of mice is considered. The persistent nature of the infection may in part contribute to the high prevalence of *H. hepaticus* in both commercial and academic mouse colonies (14, 40). Similarly, *H. pylori* causes a persistent infection

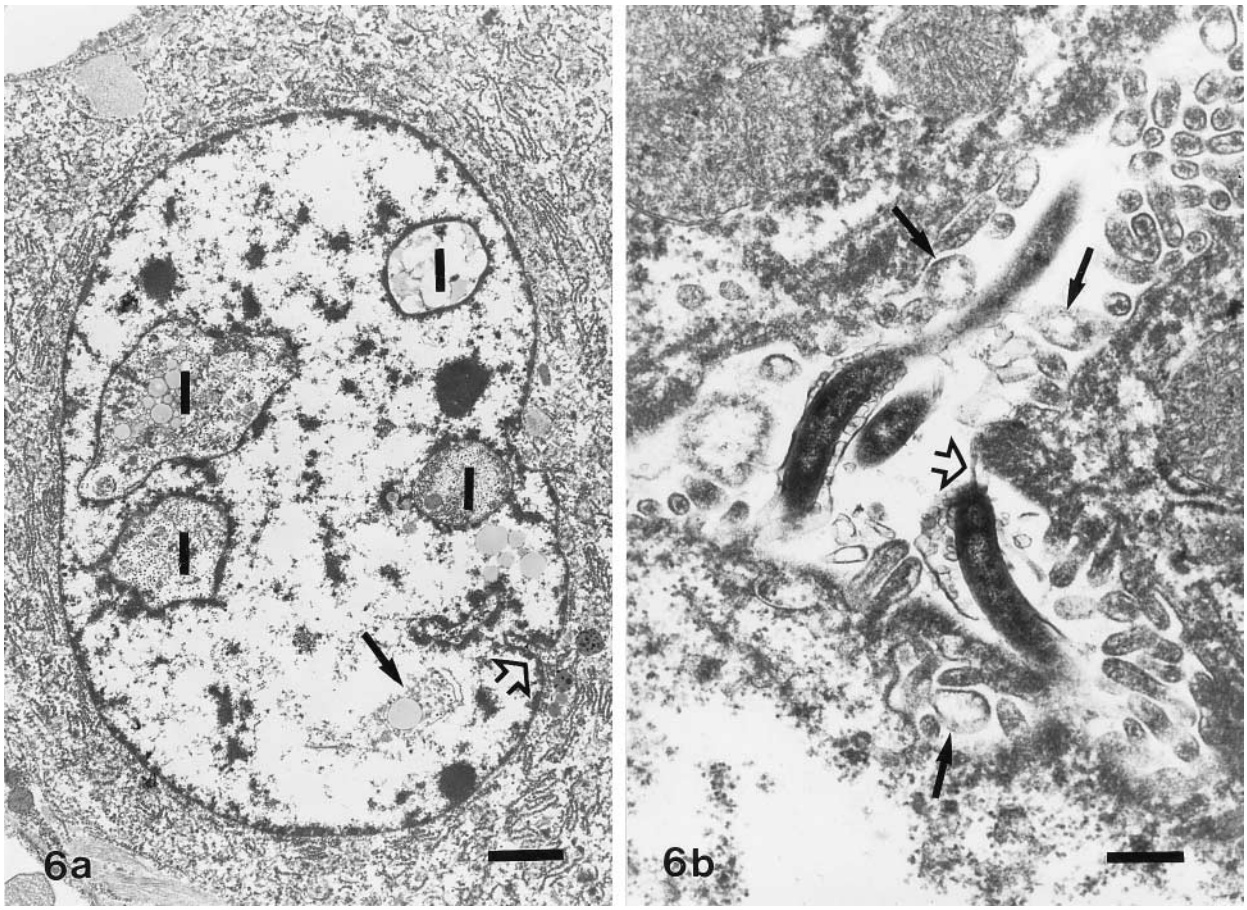

FIG. 6. (a) Liver, infected A/JCr mouse. Electron microscopy shows a hypertrophic hepatocyte with abundant rough endoplasmic reticulum in the cytoplasm and cytoplasmic invagination into the nucleus (open arrow). Intranuclear pseudoinclusions (I) have a typical cytoplasmic profile including the rough endoplasmic reticulum and lipid droplets, some of which are also free in the nucleus (arrow). Bar = 1.9 μm. (b) Liver, infected A/JCr mouse. Electron microscopy reveals the spiral-shaped *H. hepaticus* cells in a bile canaliculus, some with a flagellum (open arrow). The affected canaliculus is dilated, with swelling, blunting, and degeneration of the microvilli (solid arrows). Bar = 0.4 μm.

and induces a chronic gastritis which can exist in humans for decades (44).

Gastric helicobacter infection persists despite high sustained levels of systemic IgG antibody mounted against antigens of *Helicobacter* sp. (31). *H. hepaticus* also has apparently developed strategies to evade host immune responses similar to those of gastric helicobacters. *H. hepaticus*-infected A/JCr with hepatitis in this study had a persistent IgG antibody response to *H. hepaticus* which did not confer protection. The organism colonizes the mucous layer of intestinal crypts and bile canaliculi of the liver, both of which are ecological niches that may protect *H. hepaticus* from host defense mechanisms. Interestingly, *H. hepaticus* is also resistant to high levels of bile in vitro, which may also help explain its ability to colonize in bile canaliculi (16b). ELISA IgG serum antibodies to *H. hepaticus* are higher in male mice and in general terms correlate with the degree of hepatitis and moderate elevation of serum ALT levels seen in these animals. Younger mice colonized with *H. hepaticus* in their intestinal crypts, but without appreciable hepatitis, do not have elevated IgG *H. hepaticus* antibody or elevated ALT serum levels. These two biomarkers, therefore, may be used to measure *H. hepaticus* liver damage but are not useful for diagnosis of *H. hepaticus* intestinal infection in younger A/JCr mice.

Gastric helicobacters, such as *H. mustelae* in ferrets and *H. pylori* in humans, are known to naturally infect the host and elicit a chronic inflammation in the gastric mucosa (22, 31). Mechanisms being explored to explain this host-parasite interaction include several putative bacterial virulence factors (cytotoxins and urease, among others), which in the persistently *H. pylori*-colonized stomach probably initiate sustained production of a series of inflammatory cytokines. Urease, which produces ammonia (a tissue irritant) as a by-product of urea metabolism, is an enzyme present in high levels in *H. hepaticus* and *H. bilis* as well as gastric helicobacters (18, 21, 24, 53). The presence of these urease-producing bacteria in the liver may damage hepatocytes adjacent to the colonizing bacteria (41, 53). A vacuolating cytotoxin has been suggested, on the basis of epidemiological studies, as a potential virulence factor in *H. pylori*-induced peptic ulcer as well as *H. pylori*-associated chronic atrophic gastritis, a precancerous gastric lesion (9, 12, 19). The purified *H. pylori* exotoxin when inoculated directly into mouse stomachs induced acute gastric erosions (46). We have recently identified a soluble cytotoxin in *H. hepaticus* which produces significant cytopathic effects in vitro in a murine hepatic cell line (44, 45). It will be important to study the effects of purified *H. hepaticus* cytotoxin on mouse livers and compare the findings with those noted in livers of naturally *H. hepaticus*-infected mice.

The particulate antigen-antibody complexes noted in *H. hepaticus*-infected mouse livers by immunofluorescence appear

specific, but we do not know whether the polyclonal *H. hepaticus* antibody is directed at *H. hepaticus* antigens per se (lipopolysaccharide [LPS], urease, cytotoxin, and heat shock proteins, among others) or is reflective of antigenic mimicry between *H. hepaticus* and murine hepatocytes. For example, a possible analogy is the recent finding which indicates that Guillain-Barré syndrome may be in part an autoimmune disease which in some cases is linked directly to infection with specific *C. jejuni* serotypes, particularly serotype 19 (30). In vitro studies have demonstrated molecular homology to subunits of the LPS of *C. jejuni* and neuronal gangliosides (51, 55). Investigators also have suggested that *H. pylori* gastric-induced pathology may be in part due to autoimmunity. Several monoclonal antibodies raised against *H. pylori* have shown variable cross-reactivity against human gastric mucosa (36). Also, in a series of patients undergoing gastroscopy, the presence of seropositivity against *H. pylori* was strongly correlated with the presence of autoantibodies against human gastric mucosa. This activity was neutralized after absorption of the sera with *H. pylori* but not with other gram-negative bacteria. In addition, mice immunized with *H. pylori* also developed autoantibodies which reacted with gastric epithelium, and the stomachs of mice bearing hybridomas secreting a cross-reacting antibody had histopathologic abnormalities, although this consisted mostly of a very mild, superficial gastritis (35).

The liver lesion present in naturally *H. hepaticus*-infected mice progressively increases in severity. It is an inflammatory and necrotizing lesion which involves the hepatic parenchyma, the portal triads, and importantly, the small intralobular hepatic venules. This particular vascular involvement has not been specifically addressed previously in mice with *H. hepaticus* infection (48, 50). The widespread multifocal hepatitis and single cell to coalescing hepatocellular necrosis appeared to be random in distribution. However, these foci commonly surround the intralobular venules. Despite the presence of inflammatory lesions affecting the central veins and intralobular venules, microthrombosis was not a feature of the lesion. Microthrombosis, however, is a prominent feature of nonspecific hepatic necrosis seen in a variety of inbred strains of mice (42). Within both the parenchymal perivascular lesion and the affected portal triads, variable degrees of oval, Ito, and Kupffer cell hyperplasia were present. The mononuclear inflammatory cells occupied the connective tissue of the portal triad and extended outward to involve the adjacent hepatic parenchyma, producing necrosis and loss of hepatocytes. Inflammation of the central vein itself, including intramural mononuclear cell infiltrates and hypertrophied reactive endothelial cells, indicated the angiocentric nature of the lesion. The presence of *Helicobacter*-specific fluorescent staining within the walls of central veins further substantiated the vascular component of the lesion. Whether the vascular lesion is initiated by antigens of *H. hepaticus* is unknown, but the presence of *H. hepaticus* in the crypts of the lower bowel could allow constant low levels of soluble antigens to gain access to the portal circulation.

With BrdU, an increased liver cell proliferation associated with *H. hepaticus* was noted. There was an age-associated increase in cell proliferation in infected animals which was not seen in uninfected control mice. Similar results were seen with use of a monoclonal antibody to proliferating cell nuclear antigen (48). Although the authors did not adjust for the number of cells in a high-powered field, they also observed an age-associated increase in liver cell proliferation in mice infected with *H. hepaticus* (48). Our study investigated this observation further and demonstrated a different pattern of proliferation associated with age. Thirteen-month-old mice infected with *H. hepaticus* had both an increased number of labeled cells and a

TABLE 1. Hepatocyte proliferation in control mice and mice infected with *H. hepaticus* at 8, 10, and 13 months[a]

Group	Mean no. of cells/HPF ± SD					Mean no. of labeled cells/HPF ± SD					Mean LI% ± SD				
	All lobes	Caudate lobe	Right middle lobe	Right lateral lobe	Left lateral lobe	All lobes	Caudate lobe	Right middle lobe	Right lateral lobe	Left lateral lobe	All lobes	Caudal lobe	Right middle lobe	Right lateral lobe	Left lateral lobe
8 mo															
Control	113 ± 37	121 ± 41	109 ± 39	116 ± 43	112 ± 34	1.73 ± 0.4	1.83 ± 0.6	1.71 ± 0.4	1.80 ± 0.4	1.62 ± 0.6	1.54 ± 0.5	1.61 ± 0.6	1.56 ± 0.6	1.55 ± 0.6	1.44 ± 0.8
Infected with *H. hepaticus*	112 ± 34	113 ± 38	111 ± 37	114 ± 44	110 ± 36	2.88 ± 2.0	3.16 ± 2.6	2.60 ± 0.6	3.75 ± 4.6	2.47 ± 1.4	2.65 ± 1.2	2.83 ± 1.6	2.35 ± 1.2	3.23 ± 2.3	2.3 ± 0.8
10 mo															
Control	112 ± 32	116 ± 27	121 ± 33	122 ± 24	113 ± 20	1.21 ± 0.1	1.26 ± 0.3	1.21 ± 0.3	1.24 ± 0.3	1.17 ± 0.1	1.09 ± 0.5	1.10 ± 0.3	1.09 ± 0.4	1.01 ± 0.3	1.04 ± 0.3
Infected with *H. hepaticus*	116 ± 27	121 ± 31	118 ± 25	118 ± 28	116 ± 25	3.42 ± 1.4	4.43 ± 3.0	2.97 ± 1.3	3.10 ± 1.0	3.04 ± 1.3	2.95 ± 1.2[b]	3.65 ± 2.8	2.52 ± 1.2	2.63 ± 1.1	2.62 ± 1.9
13 mo															
Control	111 ± 29	113 ± 34	117 ± 30	106 ± 37	112 ± 31	1.45 ± 0.3	1.60 ± 0.4	1.43 ± 0.4	1.31 ± 0.2	1.41 ± 0.4	1.31 ± 0.4	1.45 ± 0.3	1.25 ± 0.5	1.29 ± 0.5	1.25 ± 0.4
Infected with *H. hepaticus*	74.5 ± 23[c]	73 ± 26	76 ± 23	77 ± 24	78 ± 22	2.93 ± 1.7	3.01 ± 1.8	2.69 ± 1.4	3.53 ± 2.4	2.77 ± 1.7	3.94 ± 2[d]	4.16 ± 2.0	3.50 ± 1.8	4.58 ± 3.2	3.56 ± 2.6

[a] All study groups consisted of 10 mice. A minimum of five high-powered fields (HPF) per lobe and a minimum of 20 high-powered fields for the total indices were assessed in each mouse. The area of the high-powered field remained constant during the experiment.
[b] $P = 0.03$ compared with controls.
[c] $P < 0.05$ compared with controls and infected mice at 8 and 10 months.
[d] $P = 0.005$ compared with controls.

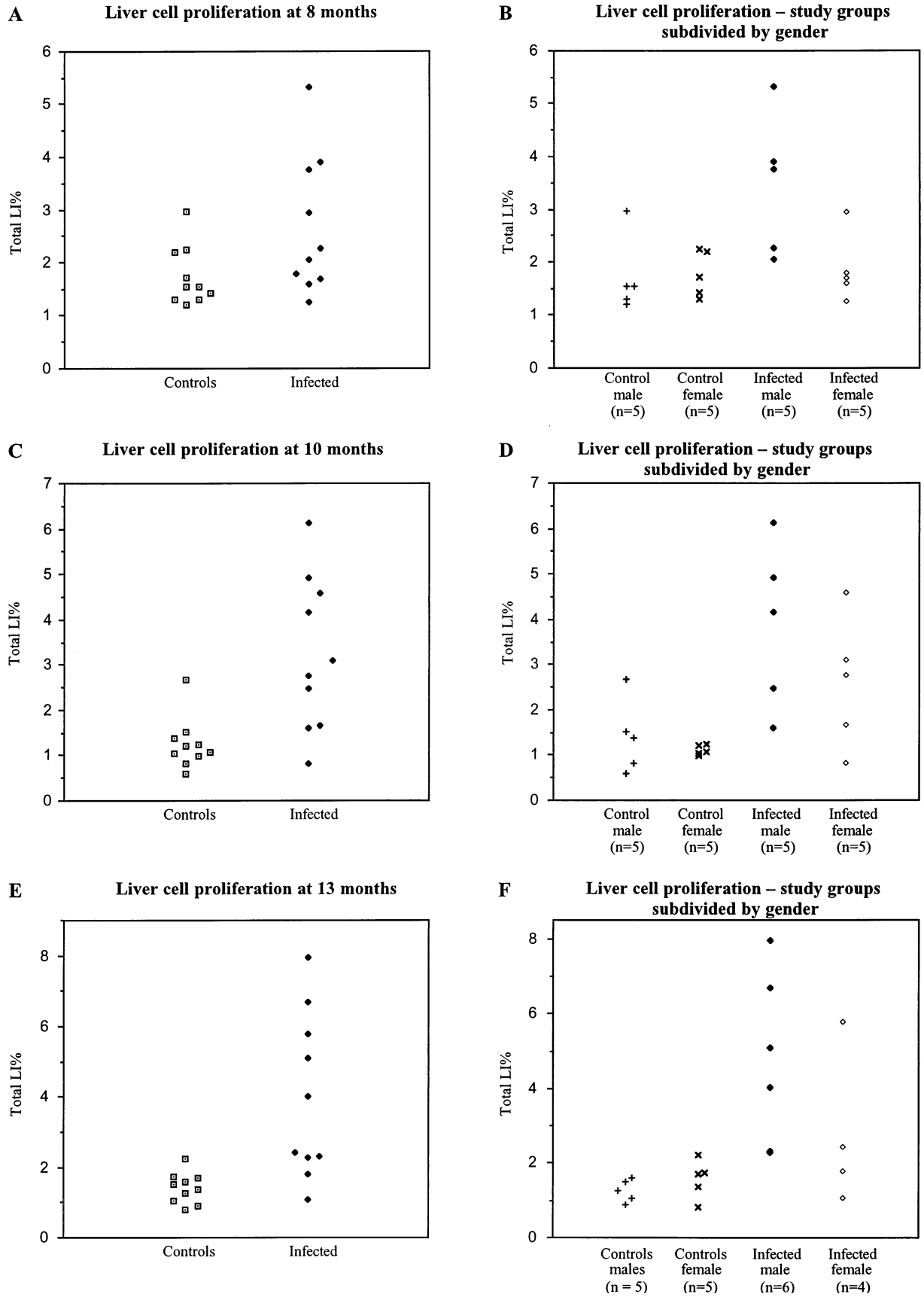

FIG. 7. Liver cell proliferation in mice infected with *H. hepaticus* and in control mice subdivided by age (8, 10, and 13 months; A, C, and E) and gender (B, D, and F).

TABLE 2. Demonstration of *H. hepaticus* antigen-antibody complex by *H. hepaticus* fluorescence-labeled polyclonal rabbit antisera

Mouse and condition	*H. hepaticus* antigen-antibody complex	*H. hepaticus*
94-475 (3 mo old)		
Before absorption	Mild	+
Absorbed once	Mild	+
Absorbed twice	Absent	−
94-574 (6 mo old)		
Before absorption	Mild	−
Absorbed once	Minimal	−
Absorbed twice	Absent	−
94-1424 (8 mo old)		
Before absorption	Moderate	+
Absorbed once	Mild	+
Absorbed twice	Absent	−
94-1187 (10 mo old)		
Before absorption	Moderate	+
Absorbed once	Mild	+
Absorbed twice	Absent	−
94-845 (12 mo old)		
Before absorption	Severe	+
Absorbed once	Mild	+
Absorbed twice	Absent	−
94-1097 (13 mo old)		
Before absorption	Moderate	+
Absorbed once	Mild	+
Absorbed twice	Absent	−
94-1621, 1657, 1658, 1660, 1661 (18 mo old)		
Before absorption	Moderate	+
Absorbed once	Minimal	−
Absorbed twice	Absent	−

decrease in total liver cells per high-powered field compared with younger infected animals. Whereas earlier studies were confined to male mice (48), our study assessed the influence of gender on liver cell proliferation in mice infected with *H. hepaticus*. Liver cell proliferation was more pronounced in male mice than in age-matched female mice. Higher rates of gastric proliferation measured by either proliferating cell nuclear antigen or BrdU have also been noted in humans infected with *H. pylori*, ferrets infected with *H. mustelae*, and C57BL mice infected with *H. felis* than in their unaffected counterparts (3, 4, 23, 54).

The increased levels of hepatocyte proliferation indices in *H. hepaticus*-infected male mice are consistent with the observation of increased hepatomas and hepatocellular carcinomas previously observed in *H. hepaticus*-infected aged A/JCr male mice (48, 50). Human males in many areas of Southeast Asia and Africa also are predisposed to hepatocellular carcinoma as a result of persistent hepatitis B virus infection (29). In this study, adenomatous nodules were noted in small numbers of 15- to 18-month-old male mice but not in female mice. Although all aged male mice in our study had hepatitis, the incidence of hepatic tumors at 15 to 18 months was 75% (3 of 4), compared with the 92% (11 of 12) incidence noted in the initial morphological observation of *H. hepaticus*-associated liver tumors in 18-month-old male mice (50). The apparent ability of *H. hepaticus* to induce hepatic neoplasms in A/JCr mice mirrors increasing epidemiological evidence that *H. pylori* can act as a cocarcinogen in development of gastric adenocarcinoma (37, 38, 43).

As information is accumulated on novel *Helicobacter* spp. and their ability to cause premalignant or malignant lesions in different animal species, it is important to note that susceptibility to cancer development is believed to be determined to a large extent by host genetic factors. This is illustrated by the susceptibility of A/JCr mice to *H. hepaticus*-associated liver tumors in contrast to some strains of mice which do not appear to be prone to *H. hepaticus*-associated hepatic lesions, e.g., C57/BL. Paralleling these observations, host genotype appears to play a role in *H. felis*-induced gastritis in mice. While SJL and C3H inbred strains and outbred Swiss mice develop a chronic gastritis due to *H. felis* infection (18, 32, 39), they do not develop the severe adenomatous and cystic hyperplasia of the gastric epithelia seen in C57/BL mice infected with *H. felis* (23). The recent publication noting a high rate of low-grade gastric lymphoma in aged (>24 months) BALB/c mice experimentally infected with *H. felis* supports the hypothesis that *Helicobacter* infection can induce different types of tumors but also demonstrates the effect of host genotypes on the type of tumor elicited by persistent *Helicobacter* infection (11).

In this study as noted previously, several A/JCr mice had a mild to moderate typhlitis (48). Typhlitis, inflammation, and proliferation of the lower bowel seen clinically as prolapse rectum have also been observed in colonies of SCID and nude mice as well as specific knockout mice with inflammatory bowel disease infected with *H. hepaticus* (13, 49). Not only did germfree outbred mice persistently infected with *H. hepaticus* for more than 2 years develop a chronic hepatitis, but in several mice a panenteritis or colitis was present (16a). Ongoing studies will help elucidate the influence of host genotype on expression of *H. hepaticus*-induced gastrointestinal and hepatic disease in mice and determine whether specific environmental factors also play a role in the progression of the disease and influence the oncogenic potential of this novel bacterium in specific strains of mice.

ACKNOWLEDGMENTS

We thank Jennifer Campbell, Allison Hayward, Nancy Taylor, and Zhao Zhibo for technical assistance.

This work was supported by grants RR07036 and RR01046 from the National Center for Research Resources and by grant R01-CA67529 and contract RFPS 94-69 from the National Cancer Institute.

REFERENCES

1. **Bayerdörffer, E., A. Neubauer, B. Rudolph, C. Thiede, N. Lehn, S. Eidt, M. Stolte, and the MALT Lymphoma Study Group.** 1995. Regression of primary gastric lymphoma of mucosa-associated lymphoid tissue type after cure of *Helicobacter pylori* infection. Lancet **345:**1591–1594.
2. **Blaser, M. J.** 1992. *Helicobacter pylori*: its role in disease. Clin. Invest. Dis. **15:** 386–393.
3. **Brenes, F., B. Ruiz, P. Correa, F. Hunter, T. Rhamakrishnan, E. Fontham, and T.-Y. Shi.** 1993. *Helicobacter pylori* causes hyperproliferation of the gastric epithelium: pre- and post-eradication indices of proliferating cell nuclear antigen. Am. J. Gastroenterol. **88:**1870–1875.
4. **Cahill, R. J., S. Sant, S. Beattie, H. Hamilton, and C. O'Morain.** 1994. *Helicobacter pylori* and increased epithelial cell proliferation: a risk factor for cancer. Eur. J. Gastroenterol. Hepatol. **6:**1123–1127.
5. **Chisari, F. V., P. Filippi, and J. Buras.** 1987. Structural and pathological effects of synthesis of hepatitis B virus large envelope polypeptide in transgenic mice. Proc. Natl. Acad. Sci. USA **84:**6909–6913.
6. **Correa, P.** 1992. Human gastric carcinogenesis: a multistep and multifactorial process. First American Cancer Society Award Lecture on Cancer Epidemiology and Prevention. Cancer Res. **52:**6735–6740.
7. **Correa, P., and J. G. Fox.** 1994. Gastric cancer and *Helicobacter pylori*, p. 239–243. *In* J. M. Pajares, A. S. Pena, and P. Malfertheiner (ed.), *Helicobacter pylori* and gastroduodenal pathology. Springer-Verlag, New York.
8. **Correa, P., J. G. Fox, E. Fontham, B. Ruiz, Y. Lin, D. Zavala, N. S. Taylor, D. Mackinley, E. de Lima, H. Portilla, and G. Zarama.** 1990. *Helicobacter pylori* and gastric carcinoma: serum antibody prevalence in populations with contrasting cancer risks. Cancer **66:**2569–2574.
9. **Cover, T. L., W. Puryear, G. I. Perez-Perez, and M. J. Blaser.** 1991. Effect of urease on HeLa cell vacuolation induced by *Helicobacter pylori* cytotoxin. Infect. Immun. **59:**1264–1270.
10. **Eldridge, S. R., T. L. Goldsworthy, J. A. Popp, and B. E. Butterworth.** 1992. Mitogenic stimulation of hepatocellular proliferation in rodents following 1,4-dichlorobenzene administration. Carcinogenesis **13:**409–415.

11. **Enno, A., J. L. O'Rourke, C. R. Howlett, A. Jack, M. F. Dixon, and A. Lee.** 1995. MALToma-like lesions in the murine gastric mucosa after long-term infection with *Helicobacter felis*. Am. J. Pathol. **147:**217–222.
12. **Figura, N., P. Guglielmetti, A. Rossolini, A. Barberi, G. Cusi, R. A. Musmanno, M. Russi, and S. Quaranta.** 1989. Cytotoxin production by *Campylobacter pylori* strains isolated from patients with peptic ulcers and from patients with chronic gastritis only. J. Clin. Microbiol. **27:**225–226.
13. **Foltz, C. J., J. G. Fox, R. J. Cahill, J. C. Murphy, L. Yan, B. Shames, and D. B. Schauer.** Possible role for *Helicobacter hepaticus* in spontaneous inflammatory bowel disease in specific mutant mouse strains. Submitted for publication.
14. **Foltz, C. J., J. G. Fox, L. Yan, and B. Shames.** 1995. Evaluation of antibiotic therapies for eradication of *Helicobacter hepaticus*. Antimicrob. Agents Chemother. **39:**1292–1294.
15. **Forman, D., D. G. Newell, F. Fullerton, J. W. Yarnell, A. R. Stacey, N. Wald, and F. Sitas.** 1991. Association between infection with *Helicobacter pylori* and risk of gastric cancer: evidence from a prospective investigation. Br. Med. J. **302:**1302–1305.
16. **Forman, D., P. Webb, D. Newell, M. Coleman, D. Palli, H. Moeller, K. Hengels, J. Elder, and G. De Backer.** 1993. An international association between *Helicobacter pylori* infection and gastric cancer. Lancet **341:**1359–1362.

16a. **Fox, J., et al.** Unpublished data.

16b. **Fox, J., and L. Yan.** Unpublished data.

17. **Fox, J. G., K. A. Andrutis, and J. Yu.** 1994. Animal models for *Helicobacter*-induced gastric and hepatic cancer, p. 504–522. *In* R. H. Hunt and G. N. J. Tytgat (ed.), *Helicobacter pylori*: basic mechanisms to clinical cure. Kluwer Academic Publishers, Boston.
18. **Fox, J. G., M. Blanco, J. C. Murphy, N. S. Taylor, A. Lee, Z. Kabok, and J. Pappo.** 1993. Local and systemic immune responses in murine *Helicobacter felis* active chronic gastritis. Infect. Immun. **61:**2309–2315.
19. **Fox, J. G., P. Correa, N. S. Taylor, N. Thompson, E. Fontham, F. Janney, M. Sobhan, B. Ruiz, and F. Hunter.** 1992. High prevalence and persistence of cytotoxin positive *Helicobacter pylori* strains in a population with high prevalence of atrophic gastritis. Am. J. Gastroenterol. **87:**1554–1560.
20. **Fox, J. G., P. Correa, N. S. Taylor, D. Zavala, E. Fontham, F. Janney, E. Rodriguez, F. Hunter, and S. Diavolitsis.** 1989. *Campylobacter pylori*-associated gastritis and immune response in a population at high risk of gastric carcinoma. Am. J. Gastroenterol. **89:**775–778.
21. **Fox, J. G., F. E. Dewhirst, J. G. Tully, B. J. Paster, L. Yan, N. S. Taylor, M. J. Collins, Jr., P. L. Gorelick, and J. M. Ward.** 1994. *Helicobacter hepaticus* sp. nov., a microaerophillic bacterium isolated from livers and intestinal mucosal scrapings from mice. J. Clin. Microbiol. **32:**1238–1245.
22. **Fox, J. G., and A. Lee.** 1993. Gastric helicobacter infection in animals: natural and experimental infections, p. 407–430. *In* C. S. Goodwin and B. W. Worsley (ed.), Biology and clinical practice. CRC Press, Boca Raton, Fla.
23. **Fox, J. G., X. Li, R. J. Cahill, K. A. Andrutis, A. K. Rustgi, R. Odze, and T. C. Wang.** 1996. Hypertrophic gastropathy in *Helicobacter felis* infected wildtype C57Bl/6 mice and p53 hemizygous transgenic mice. Gastroenterology **110:** 155–166.
24. **Fox, J. G., L. Yan, F. E. Dewhirst, B. J. Paster, B. Shames, J. C. Murphy, A. Hayward, J. C. Belcher, and E. N. Mendes.** 1995. *Helicobacter bilis* sp. nov., a novel *Helicobacter* isolated from bile, livers, and intestines of aged, inbred mouse strains. J. Clin. Microbiol. **33:**445–454.
25. **Graham, D. Y.** 1989. *Campylobacter pylori* and peptic ulcer disease. Gastroenterology **96:**615–625.
26. **Graham, D. Y., G. M. Lew, P. D. Klein, D. G. Evans, D. J. Evans, Z. A. Saeed, and H. M. Malaty.** 1992. Effect of treatment of *Helicobacter pylori* infection on the long-term recurrence of gastric or duodenal ulcer. Ann. Intern. Med. **116:**705–708.
27. **Hansson, L., L. Engstrand, O. Nyren, D. J. Evans, Jr., A. Lindgren, R. Bergström, B. Andersson, L. Athlin, O. Bendtsen, and P. Tracz.** 1993. *Helicobacter pylori* infection: independent risk indicator of gastric adenocarcinoma. Gastroenterology **105:**1098–1103.
28. **Hentschel, E., G. Brandstatter, B. Dragosics, A. M. Hirschl, H. Nemec, K. Schutze, M. Taufer, and H. Wurzer.** 1993. Effect of ranitidine and amoxicillin plus metronidazole on the eradication of *Helicobacter pylori* and the reoccurrence of duodenal ulcer. N. Engl. J. Med. **328:**308–312.
29. **Hollinger, F. B.** 1990. Hepatitis B virus, p. 2171–2236. *In* B. N. Fields and D. M. Knipe (ed.), Virology, 2nd ed. Raven Press, New York.
30. **Kuroki, S., T. Saida, M. Nukina, T. Haruta, M. Yoshioka, Y. Kobayashi, and H. Nakanishi.** 1993. *Campylobacter jejuni* strains from patients with Guillain-Barré syndrome belong mostly to Penner serogroup 19 and contain β-N-acetylglucosamine residues. Ann. Neurol. **33:**243–247.
31. **Lee, A., J. G. Fox, and S. Hazell.** 1993. The pathogenicity of *Helicobacter pylori*: a perspective. Infect. Immun. **61:**1601–1610.
32. **Lee, A., J. G. Fox, G. Otto, and J. Murphy.** 1990. A small animal model of human *Helicobacter pylori* active chronic gastritis. Gastroenterology **99:**1315–1323.
33. **Li, X., and W. L. Castleman.** 1990. Ultrastructural morphogenesis of 4-ipomeanol-induced bronchiolitis and interstitial pneumonia in calves. Vet. Pathol. **27:**141–149.
34. **Marshall, B. J., and J. R. Warren.** 1984. Unidentified curved bacilli in the stomach of patients with gastritis and peptic ulceration. Lancet **i:**1311–1314.
35. **Negrini, R., L. Lisato, I. Zanella, L. Cavazzini, S. Gullini, V. Villanacci, C. Poiesi, A. Albertini, and S. Ghielmi.** 1991. *Helicobacter pylori* infection induces antibodies cross-reacting with human gastric mucosa. Gastroenterology **101:**437–445.
36. **Negrini, R., L. Lisato, I. Zanella, P. Maini, S. Gullini, O. Basso, G. Lanza, Jr., M. Garofalo, and J. Nenci.** 1989. Monoclonal antibodies for specific immunoperoxidase detection of *Campylobacter pylori.* Gastroenterology **96:**414–420.
37. **Nomura, A., G. N. Stemmermann, P.-H. Chyou, I. Kato, G. I. Perez-Perez, and M. J. Blaser.** 1991. *Helicobacter pylori* infection and gastric carcinoma among Japanese Americans in Hawaii. N. Engl. J. Med. **325:**1132–1136.
38. **Parsonnet, J., G. D. Friedman, D. P. Vandersteen, Y. Chang, J. H. Vogelman, N. Orentreich, and R. K. Sibley.** 1991. *Helicobacter pylori* infection and the risk of gastric carcinoma. N. Engl. J. Med. **325:**1127–1131.
39. **Sakagami, T., T. Shimoyama, J. O'Rourke, and A. Lee.** 1994. Back to the host: severity of inflammation induced by *Helicobacter felis* in different strains of mice. Am. J. Gastroenterol. **89:**1345. (Abstract 241.)
40. **Shames, B., J. G. Fox, F. E. Dewhirst, L. Yan, Z. Shen, and N. S. Taylor.** 1995. Identification of widespread *H. hepaticus* infection in feces in commercial mouse colonies by culture and PCR assay. J. Clin. Microbiol. **33:**2968–2972.
41. **Smoot, D. T., H. L. T. Mobley, G. R. Chippendale, J. F. Lewison, and J. H. Resau.** 1990. *Helicobacter pylori* urease activity is toxic to human gastric epithelial cells. Infect. Immun. **58:**1992–1994.
42. **Sundberg, J. P., J. G. Fox, J. M. Ward, and H. G. Bedigian.** Idiopathic focal hepatic necrosis in inbred laboratory mice. *In* T. C. Jones, J. A. Popp, and V. Mohr (ed.), Digestive System, 2nd ed., in press. Springer-Verlag, New York.
43. **Talley, N. J., A. R. Zinsmeister, A. Weaver, E. P. DiMagno, H. A. Carpenter, G. I. Perez-Perez, and M. J. Blaser.** 1991. Gastric adenocarcinoma and *Helicobacter pylori* infection. J. Natl. Cancer Inst. **83:**1734–1739.
44. **Taylor, D. N., and J. Parsonnet.** 1995. Epidemiology and natural history of *Helicobacter pylori* infection, p. 565–588. *In* M. J. Blaser, P. D. Smith, J. I. Ravdin, H. B. Greenberg, and R. L. Guerrant (ed.), Infections of the gastrointestinal tract. Raven Press, New York.
45. **Taylor, N. S., J. G. Fox, and L. Yan.** 1995. In-vitro hepatotoxic factor in *Helicobacter hepaticus*, *H. pylori* and other *Helicobacter* species. J. Med. Microbiol. **42:**48–52.
46. **Telford, J. L., P. Ghiara, M. Dell'Orco, M. Comanducci, D. Burroni, M. Bugnoli, M. F. Tecce, S. Censini, A. Covacci, Z. Xiang, E. Papini, C. Montecucco, L. Parente, and R. Rappuoli.** 1994. Gene structure of the *Helicobacter pylori* cytotoxin and evidence of its key role in gastric disease. J. Exp. Med. **179:**1653–1658.
47. **Tilbury, L., B. E. Butterworth, O. Moss, and T. L. Goldsworthy.** 1993. Hepatocyte cell proliferation in mice after inhalation exposure to unleaded gasoline vapor. J. Toxicol. Environ. Health **38:**293–307.
48. **Ward, J. M., M. R. Anver, D. C. Haines, and R. E. Benveniste.** 1994. Chronic active hepatitis in mice caused by *Helicobacter hepaticus*. Am. J. Pathol. **145:** 959–968.
49. **Ward, J. M., M. R. Anver, D. C. Haines, J. M. Melhorn, P. Gorelick, L. Yan, and J. G. Fox.** 1996. Inflammatory large bowel disease in immunodeficient mice naturally infected with *Helicobacter hepaticus*. Lab. Anim. Sci. **46:**15–20.
50. **Ward, J. M., J. G. Fox, M. A. Anver, D. C. Haines, C. V. George, M. J. Collins, Jr., P. L. Gorelick, K. Nagashima, M. A. Gonda, R. V. Gilden, J. G. Tully, R. J. Russell, R. E. Benveniste, B. J. Paster, F. E. Dewhirst, J. C. Donovan, L. M. Anderson, and J. M. Rice.** 1994. Chronic active hepatitis and associated liver tumors in mice caused by a persistent bacterial infection with a novel *Helicobacter* species. J. Natl. Cancer Inst. **86:**1222–1227.
51. **Wirguin, I., L. Suturkovamilosevic, P. Dellalatta, T. Fisher, R. H. Brown, and N. Latov.** 1994. Monoclonal IgM antibodies to GM1 and asialo-GM1 in chronic neuropathies cross-react with *Campylobacter jejuni* lipopolysaccharides. Ann. Neurol. **35:**698–703.
52. **Wotherspoon, A. C., C. Doglioni, T. C. Diss, P. Langxing, A. Moschini, M. de Boni, and P. G. Isaacson.** 1993. Regression of primary low-grade B-cell gastric lymphoma of mucosa-associated lymphoid tissue type after eradication of *Helicobacter pylori*. Lancet **342:**575–577.
53. **Xu, J.-K., C. S. Goodwin, M. Cooper, and J. Robinson.** 1990. Intracellular vacuolization caused by the urease of *Helicobacter pylori*. J. Infect. Dis. **161:** 1302–1304.
54. **Yu, J., R. M. Russell, R. N. Salomon, J. C. Murphy, L. S. Palley, and J. G. Fox.** 1995. Effect of *Helicobacter mustelae* infection on ferret gastric epithelial cell proliferation. Carcinogenesis **16:**1927–1931.
55. **Yuki, N., T. Taki, F. Inagaki, T. Kasama, M. Takahashi, K. Saito, S. Handa, and T. Miyatake.** 1993. A bacterium lipopolysaccharide that elicits Guillian-Barré syndrome has a GM1 ganglioside-like structure. J. Exp. Med. **178:**1771–1775.

Editor: P. E. Orndorff